Transformation of human mesenchymal stem cells increases their dependency on oxidative phosphorylation for energy production

Juan M. Funes[†‡], Marisol Quintero[‡], Stephen Henderson[†‡], Dolores Martinez[†‡§], Uzma Qureshi[¶], Claire Westwood[†‡], Mark O. Clements[†‡], Dimitra Bourboulia[†‡], R. Barbara Pedley[¶], Salvador Moncada[‡‖], and Chris Boshoff[†‡‖]

[†]Cancer Research U.K. Viral Oncology Group and [‡]Wolfson Institute for Biomedical Research, Cruciform Building, Gower Street, University College London, London WC 1E 6BT, United Kingdom; and [¶]Department of Oncology, Royal Free and University College Medical School, Rowland Hill Street, London NW3 2PF, United Kingdom

Contributed by Salvador Moncada, January 25, 2007 (sent for review December 8, 2006)

An increased dependency on glycolysis for ATP production is considered to be a hallmark of tumor cells. Whether this increase in glycolytic activity is due mainly to inherent metabolic alterations or to the hypoxic microenvironment remains controversial. Here we have transformed human adult mesenchymal stem cells (MSC) using genetic alterations as described for differentiated cells. Our data suggest that MSC require disruption of the same pathways as have been shown for differentiated cells to confer a fully transformed phenotype. Furthermore, we found that MSC are more glycolytic than primary human fibroblasts and, in contrast to differentiated cells, do not depend on increased aerobic glycolysis for ATP production during transformation. These data indicate that aerobic glycolysis (the Warburg effect) is not an intrinsic component of the transformation of adult stem cells, and that oncogenic adaptation to bioenergetic requirements, in some circumstances, may also rely on increases in oxidative phosphorylation. We did find, however, a reversible increase in the transcription of glycolytic enzymes in tumors generated by transformed MSC, indicating this is a secondary phenomenon resulting from adaptation of the tumor to its microenvironment.

adult stem cells | glycolysis | Warburg effect

It has long been considered that aerobic glycolysis is an intrinsic component of the malignant phenotype (1, 2). This view has been challenged over the years (3–6), and it remains contentious whether the increased glycolysis in cancer cells is primarily the result of transformation events or due to the hypoxic tumor microenvironment (4). However, the recent observation that $p53^{-/-}$ mice exhibit impaired mitochondrial respiration (7) and the identification of a novel p53-inducible regulator of glycolysis (8) suggest a possible link between a common genetic event in human cancer and the Warburg effect.

Most experimental models of cell transformation use murine or human adult differentiated cells. Previous work has shown that *in vitro* transformation of human differentiated cells depends upon the disruption of a limited number of regulatory pathways, including the maintenance of telomeres to confer lifespan extension, the disruption of the p53 and pRB tumor suppressor pathways, and the activation of oncogenes such as c-Myc and H-Ras allowing independence from mitogenic stimuli (9–11). Recent evidence, however, suggests that cancer is derived from tissue-specific precursor or stem cells (12–14). The transformation of such cells is therefore postulated to be a prerequisite for the development of most human malignancies (12, 15). We have now studied the transformation of mesenchymal stem cells (MSC) to test the hypothesis that adult stem cells might require fewer genetic alterations to be transformed *in vitro* compared with adult differentiated cells (16) and to determine whether the metabolic alterations that occur during MSC transformation differ from those reported in adult differentiated human cells (17).

Results

Transformation of Human MSC. Tissue-specific MSC, or mesenchymal precursor cells, are thought to be the cell of origin for various types of sarcoma (18). We therefore used human primary MSC isolated from bone marrow of a healthy donor. These cells showed the expected cell surface marker profile (Fig. 1*A*), and their multipotency was confirmed by differentiation to adipocytes, osteocytes, and chondrocytes (Fig. 1*B*). We used retroviruses encoding for the catalytic subunit of human telomerase (hTERT), HPV-16 E6 and E7, SV40 small T antigen (ST), and an oncogenic allele of H-Ras ($H\text{-}Ras^{V12}$) to induce transformation (9, 19, 20). Fig. 2*A* shows our experimental approach to transforming MSC, although various sequential combinations of these oncogenic steps or "hits" were also tested. *In vitro*, MSC have a limited proliferative potential, therefore the ectopic expression of hTERT is necessary to extend their lifespan in culture (data not shown). HPV-16 E6 and E7 abrogate the functions of p53 and pRB family members, respectively; ST inactivates protein phosphatase 2A, resulting in c-Myc stabilization (20, 21); and $H\text{-}Ras^{V12}$ provides acquisition of a constitutive mitogenic signal. The expression of introduced oncogenes or their downstream targets was confirmed by RT-PCR (data not shown), Western blot (Fig. 2*B*), or gene expression microarrays (GEM) [supporting information (SI) Fig. 6]. GEM analyses also showed that perturbation of these five pathways in MSC stepwise transformation elicited changes frequently associated with human tumor cells (22) (SI Fig. 7).

Anchorage-independent growth was tested by growing cells in soft agarose. Cells transduced with hTERT, E6, E7, and ST (4 hits) formed small colonies by day 12, whereas the addition of $H\text{-}Ras^{V12}$ (5 hits) induced rapidly growing large colonies (Fig. 2*C* and Table 1). The combination of hTERT, E6, E7, and $H\text{-}Ras^{V12}$ (4* hits) did not induce colonies after 12 days in culture.

Author contributions: S.M. and C.B. designed research; J.M.F., M.Q., D.M., U.Q., C.W., and D.B. performed research; M.O.C. and R.B.P. contributed new reagents/analytic tools; J.M.F., M.Q., S.H., S.M., and C.B. analyzed data; and J.M.F., M.Q., S.M., and C.B. wrote the paper.

The authors declare no conflict of interest.

Abbreviations: MSC, mesenchymal stem cell; hTERT, human telemorase; ST, small T antigen; GEM, gene expression microarray; PPP, pentose phosphate pathway; HF, human fibroblast; 2-DG, 2-deoxy-D-glucose; R-5-P, ribose-5-phosphate; PRPS, phosphoribosylpyrophosphate synthetase; HIF-1α, hypoxia-inducible transcription factor 1α.

Data deposition: The microarray data reported in this paper have been deposited in the ArrayExpress database [accession nos. E-MEXP-562 (MSC tumors) and E-MEXP-563 (MSC transformation)].

[§]Present address: FACS Laboratory, London Research Institute, Cancer Research U.K., Lincoln's Inn Fields, London WC2A 3PX, United Kingdom.

[‖]To whom correspondence may be addressed. E-mail: s.moncada@ucl.ac.uk or c.boshoff@ucl.ac.uk.

This article contains supporting information online at www.pnas.org/cgi/content/full/0700690104/DC1.

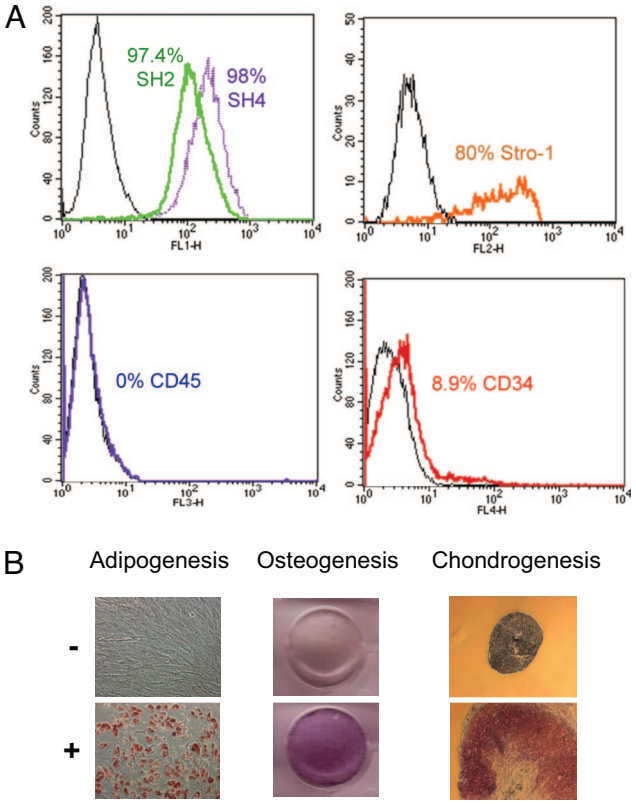

Fig. 1. Characterization of human MSC. (*A*) Isolated MSC were shown to express MSC markers including SH2, SH4, and Stro-1 as determined by FACs analysis. CD34 (hematopoietic stem cell marker) and CD45 (pan-leukocyte marker), considered to be negative mesenchymal markers, were not expressed in MSC. Control cells are also shown (black). (*B*) MSC multipotency was confirmed by differentiation (+) to adipocytes, osteocytes, and chondrocytes. Control cells, where differentiation was not induced (−), are also shown.

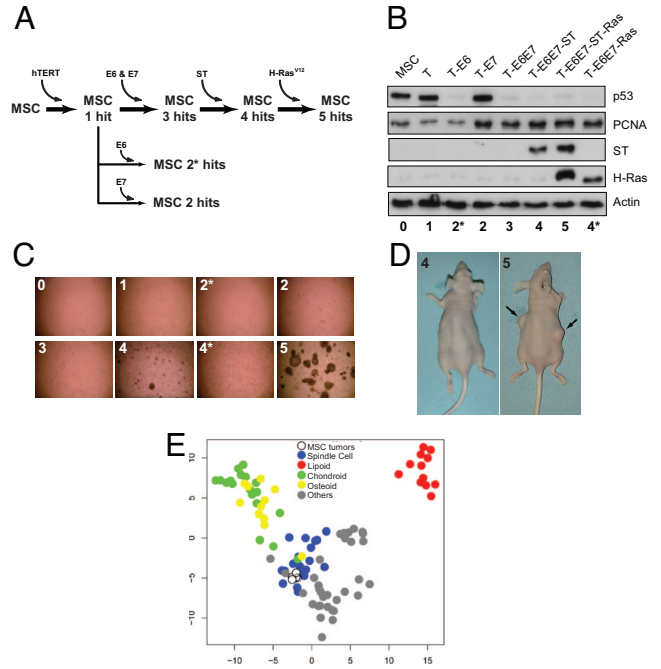

Fig. 2. Transformation of human MSC. (*A*) Schematic diagram of MSC stepwise transformation. Cell lines were named according to the number of steps or hits introduced sequentially by retroviral transduction (see Table 1). (*B*) Cell lines were probed by antibodies against introduced oncogenes or their downstream cellular targets. Proliferating cell nuclear antigen (PCNA) reflects cell entry in S phase after pRB inactivation by E7. (*C*) Anchorage-independent growth of MSC infected with empty retroviruses or combinations of different oncogenes. (*D*) Tumors formed in mice inoculated with 5 hits MSC (arrows), but not in those inoculated with 4 hits MSC (*Left*). (*E*) GEM profiles of five of the MSC tumors generated in mice (open circles) were compared with 96 human sarcomas (23). Multidimensional scale (MDS) shows that the tumors generated in mice clustered with human spindle cell sarcomas.

However, after 4 weeks, all cells expressing E7 showed colony formation in soft agarose (data not shown). This suggests that disruption of the pRB pathway is sufficient to induce anchorage-independent growth in MSC. Next, we tested the growth of the transduced MSC in immunodeficient mice. Nearly all mice inoculated with MSC transduced with 5 hits developed tumors (Fig. 2*D* and Table 1). The 4* hits cell line gave rise to tumors in 2/10 inoculation sites with a significantly longer latency than that of the 5-hits cell line (Table 1), suggesting that additional mutations might have occurred during *in vivo* growth of these cells. Our data indicate that the same genetic steps are required in MSC as in differentiated cells to confer a fully transformed phenotype.

The phenotype of the tumors originating from the 5-hits cell line was confirmed by comparing their GEM profiles to those of 96 different human sarcomas using a subset of genes previously identified as a molecular fingerprint for sarcoma (23). Multidimensional scaling demonstrated that the tumors generated in mice from MSC all cluster with the spindle-cell sarcoma group (Fig. 2*E*), implying that the *in vitro* transformation of MSC is a relevant model for human sarcoma. The tumors did not show evidence of differentiation toward other mesenchymal lineages (Fig. 2*E*).

Next, we tested the effects of transformation on MSC multipotency. All MSC lines, including transformed MSC (5 hits), still expressed the MSC-associated markers SH2, SH4, and Stro-1 but not CD45 or CD34 (data not shown and SI Fig. 8*A*). Furthermore, transformed MSC maintained their ability to undergo differentiation toward adipocytes (SI Fig. 8*B*) and chondrocytes (SI Fig. 8*C*), albeit less efficiently than primary MSC. The rapid proliferation of transformed cells, however, prevented us from determining the efficiency of differentiation toward osteocytes. These data suggest that transformation by itself does not completely abrogate the multipotency of MSC.

Bioenergetic Changes During *in Vitro* Transformation. To investigate the effects of stepwise transformation on metabolic pathways, we generated a list of genes known to play a role in cell metabolism (SI Table 3) and analyzed GEM data using only these probes. SI Fig. 9 shows the effect of sequential transformation on the

Table 1. *In vitro* and *in vivo* MSC transformation

MSC	Hits	Colonies in soft agarose	Tumors in mice/inoculation	Tumor latency, days
Parental	0	0	0/6	NA
T	1	0	0/6	NA
T-E6	2*	0	0/6	NA
T-E7	2	0	0/6	NA
T-E6E7	3	0	0/6	NA
T-E6E7-ST	4	25 ± 4	0/6	NA
T-E6E7-Ras	4*	0	2/10	69
T-E6E7-ST-Ras	5	1,729 ± 98	32/34	20–27

The number of colonies (± standard deviation) after 12 days in culture is shown. Cell lines expressing only E6, only E7, or E6 and E7 did not give rise to colonies in soft agarose or to tumors when inoculated into nude mice (data not shown). NA, not applicable.

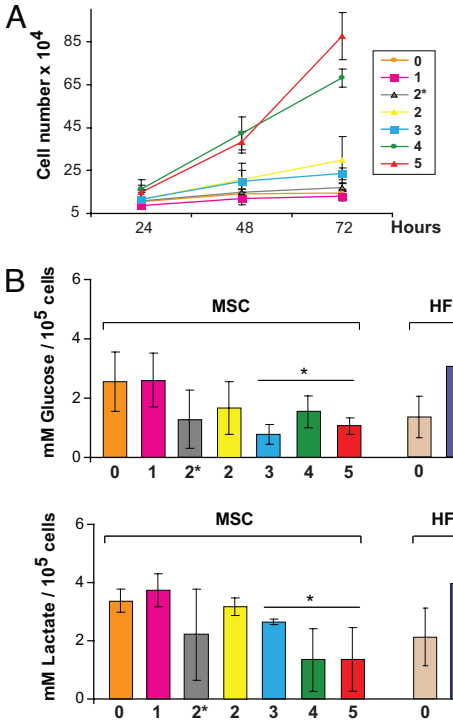

Fig. 3. Functional assays of bioenergetic pathways during stepwise transformation. (*A*) Growth curve showing the number of cells at 24, 48, and 72 h. Lanes 0–5 indicate cells with different number of genetic hits (see Table 1). (*B*) Values of glucose uptake and lactate release at 48 h corrected for cell number in MSC and HF during stepwise transformation (*, $P < 0.05$; Student's *t* test). Lanes 0–5 indicate parental cells (0) and each subsequent step in transformation.

glycolytic-, pentose phosphate- (PPP), and nucleotide synthesis pathways, and the TCA cycle. During transformation, the expression profile of glycolytic genes was not significantly altered between MSC and transformed cells (5 hits, $P = 0.27$), whereas genes in the TCA cycle showed a trend toward up-regulation ($P = 0.11$). The overall expression profile of genes in the PPP was significantly down-regulated ($P = 0.0039$), whereas genes involved in nucleotide biosynthesis were highly up-regulated ($P < 0.0001$).

We next used functional assays to explore the array data. After MSC 5 hits, there was an apparent increase in both glucose uptake and production of lactate, the end product of glycolysis (data not shown). However, the proliferative rate in MSC varies depending on the number of hits (Fig. 3*A*), and the total concentration of glucose and lactate was clearly related to cell proliferation. When corrected for cell number, there was, in fact, a significant decrease in both glucose uptake and lactate production when compared with parental MSC (Fig. 3*B*). Because this was an unexpected result, we repeated the experiments with human fibroblasts (HF). When HF were transformed using the same oncogenic elements (SI Fig. 10), we observed that both glucose uptake and lactate production were increased compared with that in parental fibroblasts (Fig. 3*B*). This is in agreement with data reporting that expression of cancer-causing genes in HF increased their dependency on glycolysis for energy production (17).

Next, we compared the contribution of both the mitochondrial and glycolytic pathways to total ATP production in transformed MSC and HF. The inhibition of mitochondrial respiration by rotenone significantly decreased ATP production in 5 hits MSC, but not in primary MSC (Table 2). This indicates that transformed MSC depend more than primary MSC on oxidative phosphorylation for energy production and contrasts with HF, which depend less on oxidative phosphorylation after transformation. Moreover, transformed HF were more sensitive to glycolysis inhibition by 2-deoxy-D-glucose (2-DG) than parental fibroblasts, whereas both MSC lines were equally affected by the addition of 2-DG.

Table 2. Effect of metabolic inhibitors on ATP concentrations

	% ATP vs. control		
	Rotenone	2-DG	Rotenone + 2-DG
MSC	97.99 ± 10.31	59.27 ± 15.59	13.38 ± 13.44
MSC 5 hits	66.67 ± 10.83*	56.14 ± 3.81	13.47 ± 7.58
HF	54.92 ± 11.85	64.24 ± 17.76	9.05 ± 5.48
HF 5 hits	74.95 ± 10.87*	48.21 ± 17.57	6.19 ± 4.25

Percent changes in ATP production after treating cells with mitochondrial (rotenone) and glycolytic (2-DG) inhibitors when compared with untreated cells (*, $P < 0.05$; Student's *t* test).

Role of PPP in Transformed MSC. Glucose can also be used by the PPP for the generation of NADPH for reductive biosynthesis or for the formation of ribose-5-phosphate (R-5-P) for the synthesis of nucleotides and nucleic acids. Confirming the GEM data for the metabolism of glucose by the PPP (SI Fig. 9), we found that the activity and protein expression of the rate-limiting glucose-6-phosphate dehydrogenase (G6PD) were down-regulated at the late stages of MSC transformation (Fig. 4*A*). We also observed a down-regulation of enzymes such as 6-phosphogluconate dehydrogenase, transketolase, and transaldolase (SI Fig. 9 and qRT-PCR, data not shown). In contrast to reports in differentiated mammalian cells (24), increased proliferation and transformation of MSC did not lead to up-regulation of the PPP. Although G6PD activity was reduced, the general trend of the

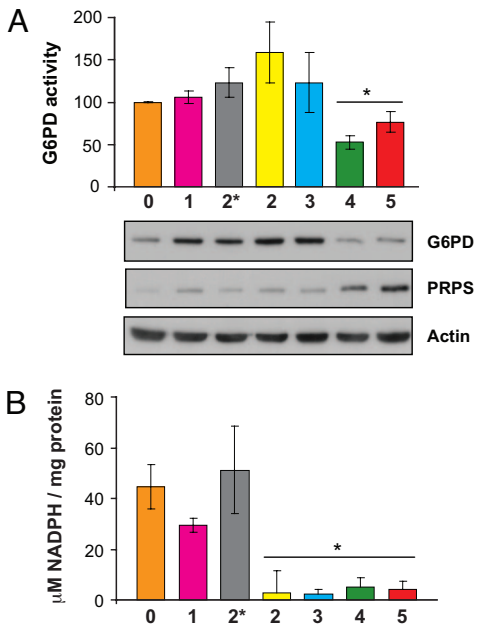

Fig. 4. Role of PPP during MSC transformation. (*A*) G6PD activity decreased during MSC transformation (*, $P = 0.0132$; *t* test). Western blot confirms the down-regulation of G6PD and the up-regulation of PRPS at the late stages of transformation. (*B*) MSC transformation also led to a significant decrease in NADPH levels (*, $P = 0.0014$; Student's *t* test).

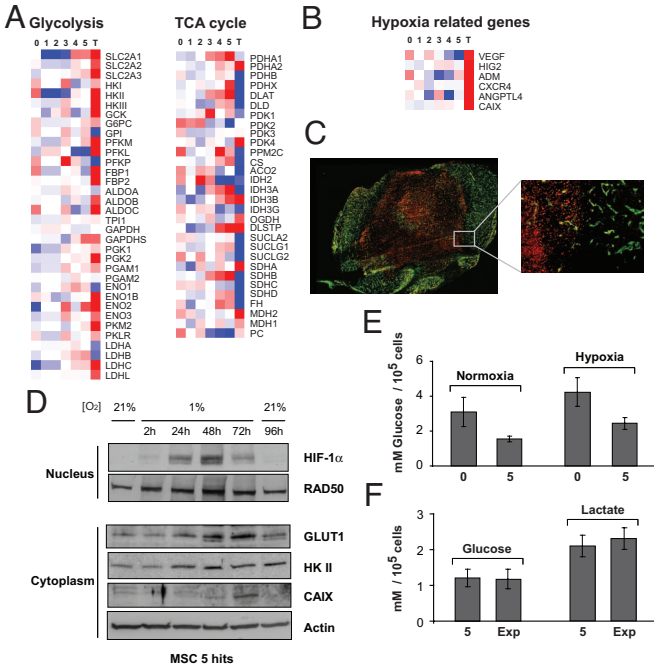

Fig. 5. Bioenergetic profiles of tumors originating from MSC *in vivo*. (*A*) The heatmaps summarize the average of three samples from cell lines (0–5) and five tumors (T) for glycolytic and TCA cycle genes (representative probes for each gene were chosen). Red indicates up-regulation, and blue down-regulation from the mean. (*B*) Hypoxia-related genes such as VEGF, hypoxia-inducible protein 2 (HIG2), adrenomedullin (ADM), chemokine CXC motif receptor 4 (CXCR4), and angiopoietin-like 4 (ANGPTL4) were up-regulated in the tumors, compared with *in vitro* transformed cells. (*C*) Immunohistochemistry for GLUT1 showed that the central poorly vascularized region of a tumor stained strongly positive (red, 24 × 26 image montage, ×200 magnification). *Inset* shows higher magnification of GLUT1 staining (red), distinct from the well vascularized region, stained with CD31 (green, 2 × 2 image montage, ×200 magnification). (*D*) Western blotting confirmed that when transformed MSC were exposed to hypoxia (1% O_2), HIF-1α, GLUT1, hexokinase II (HK II), and CAIX were up-regulated. RAD50 and actin were used as loading controls. (*E*) Values of glucose uptake at 48 h for parental (0) and 5 hits (5) MSC grown at 21% and 1% O_2. (*F*) Glucose uptake and lactate release in 5 hits MSC (5) compared with 5 hits MSC explanted from tumors (Exp) and cultured for 3 weeks.

pathway, however, was toward an increased synthesis of nucleotides (SI Fig. 9). We observed an up-regulation of ribose 5-phosphate isomerase A (RPIA) (SI Fig. 9 and qRT-PCR; data not shown), which produces R-5-P and leads to an increase in enzymes involved in DNA synthesis such as phosphoribosylpyrophosphate synthetase (PRPS) (SI Fig. 9 and Fig. 4*A*). MSC also showed a significant drop in NADPH levels correlating with an increase in cell proliferation after the introduction of E7 (2 hits) (Figs. 3*A* and 4*B*). In transformed MSC, the PPP, therefore, could be operating to generate mainly R-5-P for nucleotide synthesis and not to produce the intracellular reductant NADPH.

Bioenergetic Changes During *in Vivo* Tumor Growth. Because monolayer cultures of cells transformed *in vitro* do not reflect the 3D cellular growth of a tumor *in vivo* (25), we next compared the gene expression profiles of the tumors generated *in vivo* to those of the transduced cells. Strikingly, there was a general induction of glycolytic genes and an overall down-regulation of those in the TCA cycle in these tumors (Fig. 5*A*). In the PPP, no difference in gene expression between mouse tumors and *in vitro* transformed MSC was seen (data not shown).

In vivo, glycolysis could be a result of the hypoxic activation of hypoxia-inducible transcription factor 1α (HIF-1α) (26, 27). In mouse tumors, the GEM data showed an increase in HIF-1α -dependent genes such as glucose transporter 1 (SLC2A1 or GLUT1), carbonic anhydrase IX (CAIX), and VEGF (Fig. 5 *A* and *B*). We confirmed that GLUT1 is expressed in the central necrotic areas of the mouse tumors (Fig. 5*C*), but not, however, in well vascularized tumors (data not shown). We therefore investigated whether *in vitro* hypoxia induces the expression of glycolytic and hypoxia-related proteins in transformed MSC. Western blots confirmed HIF-1α stabilization in these cells at 1% O_2 and an increased expression of glycolytic enzymes, compared with normoxia (Fig. 5*D*). This was reversed when the cells were reexposed to 21% O_2 (Fig. 5*D*). Furthermore, we observed a significant increase in glucose uptake ($P < 0.005$, t test) when parental MSC and those with 5 hits were exposed to hypoxia (Fig. 5*E*).

To test whether this glycolytic switch observed *in vivo* was reversible, cells obtained from mouse tumors were cultured for 3 weeks at 21% O_2 and assayed for glucose uptake and lactate release. The explanted cells consumed similar levels of glucose and produced amounts of lactate similar to those observed in *in vitro* transformed MSC (5 hits) (Fig. 5*F*). Furthermore, ATP production after treatment with rotenone and 2-DG was similar in explanted cells compared with 5 hits (data not shown), suggesting that the tumors generated in mice reversed their glycolytic phenotype when explanted and grown in culture.

Discussion

We have shown that transformation of MSC requires the alteration of the same pathways described for differentiated adult cells and in itself does not completely abrogate their multipotency. Furthermore, during transformation, MSC not only do not switch to aerobic glycolysis, but their dependency on oxidative phosphorylation is increased.

It has been proposed that the intrinsic properties of normal adult stem cells might result in a requirement for fewer or different steps than differentiated cells to acquire a transformed phenotype (16). Moreover, it has been reported that spontaneous transformation of primary and telomerase-immortalized MSC isolated from adipose tissue and bone marrow occurs after long-term culture *in vitro* (28, 29). However, our data indicate that MSC require the same number of steps to achieve transformation as have been shown for differentiated cells, suggesting that properties of self-renewal and multipotency might not necessarily assist in the transformation process. This discrepancy with the previous reports could be due to the different origin of the MSC samples such as tissue or donor or to the different culture conditions, including the longer periods of *in vitro* growth that could make these cells more prone to developing spontaneous mutations.

Various factors have been suggested to contribute to the glycolytic switch occurring in differentiated cells during transformation. These include inhibition of oxidative phosphorylation due to defects in mitochondrial DNA (30) or a dysfunctional TCA cycle (31), the activation of various oncogenes and tyrosine kinase pathways including c-Myc (32), Ras (17, 33), SRC (33), and AKT (2), the inactivation of p53 (7, 8) and a low-oxygen tumor microenvironment, resulting in the activation of hypoxia-inducible transcription factors (26, 27). Our results suggest that these changes might be cell-specific, and that MSC do not respond to transformation by an increased cell dependency on glycolysis as differentiated cells do. It is likely that some cells may adapt to neoplastic transformation by increasing their dependency on oxidative phosphorylation (34).

We observed a clear increase in glycolysis and in the expression of glycolytic enzymes only when transformed MSC were grown as tumors in mice, or when the cells were exposed to a hypoxic environment *in vitro*. These changes were reversible and

did not occur in highly vascularized tumors, indicating they are adaptive and depended on the hypoxic environment. Whether this glycolytic switch is always reversible, or whether at some point these changes become a permanent component of the neoplastic transformation, as was suggested many years ago (35), remains to be investigated.

Contrary to reports suggesting that G6PD is increased in human cancer (36) and could play a role in cell transformation (37), our transformed MSC showed a decrease in G6PD levels and activity. However, there was a clear shunting of the pathway toward R-5-P and the synthesis of nucleotides, as shown by the increase in RPIA and PRPS. This occurred in the presence of decreased amounts of NADPH. Because a decrease in NADPH would affect the synthesis of the antioxidant glutathione, this might contribute to the well documented increase in reactive oxygen species and the prooxidant nature of cancer cells (38). It is worth noting that, in spite of the fact that G6PD levels remained high after 2 and 3 hits (Fig. 4*A*), the concentrations of the NADPH were significantly reduced (Fig. 4*B*) at these stages. This could be explained by the increased consumption of NADPH required to support the increased cell proliferation observed. This requires further investigation.

Our results indicate that the transformation of human adult stem cells such as MSC leads to different bioenergetic changes from those of differentiated cells. If adult tissue-specific stem cells are the origin of most cancers (13), then the assumption that aerobic glycolysis is part of the neoplastic transformation needs to be critically reviewed. The well known increase in glucose uptake in tumors (5, 39) may, in fact, be explained by the enhanced cell proliferation and the response to hypoxia, acting in concert. Our observations should now be extended to other putative cancer stem cells, to establish their dependency on glycolysis and the bioenergetic changes occurring during transformation.

Experimental Procedures

MSC Isolation, Phenotype, and Cell Culture. Bone marrow mononuclear cells derived from a healthy 34-year-old male donor were isolated by density gradient centrifugation (Ficoll, Amersham Biosciences, Bucks, U.K.) and resuspended in Mesencult medium containing 10% human serum (StemCell Technologies, Vancouver, Canada; catalog nos. 05401 and 05402) and 1 $ng{\cdot}ml^{-1}$ basic fibroblast growth factor (R&D Systems, Minneapolis, MN; catalog no. 233-FB). Two days after plating, nonadherent cells were removed and fresh medium added. MSC colonies formed after plating were designated as passage 0 and maintained in this medium. Cells were kept at subconfluent levels and passaged every 3 days, with the first passage occurring at approximately day 7 after isolation.

For immunophenotyping of MSC, samples were incubated with the following antibodies: anti FITC SH2 and SH4 (Stem Cell Technologies), anti-PECy7 CD45 and anti-APC CD34 (Pharmingen, San Diego, CA), Stro-1 (R&D Systems), and PE anti-mouse IgM (Caltag, CA). Ten thousand events from the alive gate were collected in a FACS Calibur instrument (BD Biosciences, San Jose, CA) equipped with 488- and 635-nm lines. Data were analyzed by using CellQuest V software. Dead cells were excluded from the analysis by using propidium iodide or 7-amino-actinomycin D.

Retrovirus production and infection of target cells were carried out as described (40). The retroviral vectors used were: $pMarX_{IV}$-hygro-eGFP, pBABE-puro-EST2 (hTERT), pLXSN-neo-E6, pLXSN-neo-E7, pLXSN-neo-E6E7, pBABE-zeo-ST, and pWZL-hygro-Ras^{V12} [from D. Beach (Institute for Cell and Molecular Sciences, London, U.K.) and R. Weinberg (Whitehead Institute for Biomedical Research, Cambridge, MA)]. Retroviral constructs were introduced serially, and drug selection was used to purify cell populations between infections. Cells were selected in puromycin (1 $\mu g{\cdot}ml^{-1}$), neomycin (300 $\mu g{\cdot}ml^{-1}$), zeocin (50 $\mu g{\cdot}ml^{-1}$), or hygromycin (100 $\mu g{\cdot}ml^{-1}$), respectively. Retroviral vectors carrying only drug-resistant genes were also used as controls. Alternatively, retroviral supernatants were produced by cotransfection of 293gp cells (Clontech, Saint-Germain-en-Laye, France) with retroviral plasmids and pMDG (encodes VSVG envelope protein) using lipofectamine (Invitrogen, Paisley, U.K.).

Hypoxia (1% oxygen) was achieved by incubation of the cells at 37°C in an oxygen-controlled hypoxic chamber (Coy Laboratory Products, Ann Arbor, MI) for 2, 24, 48, and 72 h.

HF and the packaging cell line LinX-A (provided by D. Beach) were grown in DMEM (Gibco, Invitrogen, Paisley, U.K.) supplemented with 10% FCS.

Adipogenic, osteogenic, and chondrogenic differentiation protocols are explained in *SI Materials and Methods*.

Transformation Assays. Anchorage-independent growth was assayed by soft agarose assays. After selection with the appropriate drugs, 10^4 cells were transferred to 2 ml of medium solution (without basic fibroblast growth factor) of 0.35% low melting point agarose (Sigma, St. Louis, MO) and seeded in triplicate into six-well plates containing a 2-ml layer of solidified 0.6% agarose in medium. Fresh medium was added every 3 days and colonies photographed at ×40 magnification after 12 days in culture. For tumor formation assays, 5×10^6 cells were injected s.c. into both flanks of 6- to 8-week-old athymic CD1 nude mice (Charles River Breeding Laboratories, Wilmington, MA). Mice were culled either when at least one of the tumors reached a diameter of 1.5 cm or 6 months after inoculation. At this point, in some experiments, explanted tumors were incubated with medium containing collagenase (1 $mg{\cdot}ml^{-1}$; GIBCO) for 4 h, washed, and placed in culture under hygromycin selection.

Western Blotting. The following antibodies were used for Western blotting: sc-126 (DO-1) for p53, sc-56 (PC10) for PCNA, sc-35 (259) for H-Ras, sc-148 (Pab 108) for SV40 ST antigen, sc-17253 (N-19) for CAIX, sc-6521 (C-14) for HK II (all from Santa Cruz, Santa Cruz, CA); Ab-1 for actin (from Oncogene, Cambridge, MA); BL341 for G6PD (from Bethyl, Montgomery, TX); AP7061a antibody for PRPS1/2/3 (from Abgent); ab1932 for GLUT1 (from Abcam, Cambridge, U.K.). RAD50 and HIF1-α antibodies were both from BD Biosciences, San Diego, CA (catalog nos. 611010 and 610958, respectively).

Glucose and Lactate Measurement. Cell lines were plated in six-well dishes (4×10^4 cells per well), and the next day fresh medium was added and cells were incubated for 3 additional days (24, 48, and 72 h). Medium samples were collected each day and stored at −20°C until they were assayed. Glucose and lactate were measured using commercial kits from Sigma and Trinity Biotech (County Wicklow, Ireland), respectively. Each day, cells were counted, and the results from glucose and lactate experiments were corrected and expressed as mM per 10^5 cells. Results plotted were obtained after 48 h and are representative of at least three different experiments.

Glucose 6-Phosphate Dehydrogenase Activity. The activity of glucose 6-phosphate dehydrogenase in cell extracts was measured following the manufacturer's instructions (Trinity Biotech). Results from three independent experiments were corrected per milligram of protein and represented as a percentage of the activity in primary MSC.

NADPH. NADPH determination was carried out as described (41). Results from three independent experiments were corrected per protein content of each sample.

ATP Determination. ATP was measured by the luciferin/luciferase method by using a chemiluminescence kit (Perkin/Elmer, Bucks, U.K.), following the manufacturer's protocol. 2-DG and rotenone were purchased from Sigma.

Immunofluorescence. Tumor preparation and fluorescence microscopy were carried out as described (42). In brief, double staining for GLUT1 and blood vessels was carried out as follows: tumor sections were blocked in 3% goat serum for 20 min followed by incubation with a rat anti-mouse CD31 for blood vessels, diluted to one-half, and incubated for 1 h at room temperature. After washing in PBS, sections were simultaneously incubated with goat anti-rat Alexa fluor 488 (Invitrogen), diluted to 1/200 to detect CD31, and rabbit polyclonal GLUT1 (Dako, Cambridgeshire, U.K.), conjugated to Alexa Fluor 546 and diluted to 1/10. Sections were then incubated for 1 h at 22°C and viewed under a fluorescence microscope.

Statistics. Data were analyzed by using Student's *t* test. Values are given as mean ± SEM. A P value of <0.05 was considered statistically significant.

We thank Kwee Yong at University College Hospital for supplying the bone marrow for MSC isolation and Annie Higgs for critical reading of the manuscript. We also thank Nadege Presneau, Sonja Vujovic, Mathew Robson, and Nancy Frakich for technical help. This work was supported by Program Grants from Cancer Research U.K., the U.K. Medical Research Council, and the Wellcome Trust (Functional Genomics Initiative). M.Q. is supported by the Spanish Ministry of Health.

1. Warburg O (1956) *Science* 123:309–314.
2. Elstrom RL, Bauer DE, Buzzai M, Karnauskas R, Harris MH, Plas DR, Zhuang HM, Cinalli RM, Alavi A, Rudin CM, *et al.* (2004) *Cancer Res* 64:3892–3899.
3. Chance B, Castor LN (1952) *Science* 116:200–202.
4. Zu XL, Guppy M (2004) *Biochem Biophys Res Commun* 313:459–465.
5. Gatenby RA, Gillies RJ (2004) *Nat Rev Cancer* 4:891–899.
6. Hatzivassiliou G, Zhao FP, Bauer DE, Andreadis C, Shaw AN, Dhanak D, Hingorani SR, Tuveson DA, Thompson CB (2005) *Cancer Cell* 8:311–321.
7. Matoba S, Kang JG, Patino WD, Wragg A, Boehm M, Gavrilova O, Hurley PJ, Bunz F, Hwang PM (2006) *Science* 312:1650–1653.
8. Bensaad K, Tsuruta A, Selak MA, Vidal MN, Nakano K, Bartrons R, Gottlieb E, Vousden KH (2006) *Cell* 126:107–120.
9. Hahn WC, Counter CM, Lundberg AS, Beijersbergen RL, Brooks MW, Weinberg RA (1999) *Nature* 400:464–468.
10. Hahn WC, Weinberg RA (2002) *N Engl J Med* 347:1593–1603.
11. Rangarajan A, Hong SJ, Gifford A, Weinberg RA (2004) *Cancer Cell* 6:171–183.
12. Reya T, Morrison SJ, Clarke MF, Weissman IL (2001) *Nature* 414:105–111.
13. Bjerkvig R, Tysnes BB, Aboody KS, Najbauer J, Terzis AJ (2005) *Nat Rev Cancer* 5:899–904.
14. Polyak K, Hahn WC (2006) *Nat Med* 12:296–300.
15. Beachy PA, Karhadkar SS, Berman DM (2004) *Nature* 432:324–331.
16. Vitale-Cross L, Amornphimoltham P, Fisher G, Molinolo AA, Gutkind JS (2004) *Cancer Res* 64:8804–8807.
17. Ramanathan A, Wang C, Schreiber SL (2005) *Proc Natl Acad Sci USA* 102:5992–5997.
18. Helman LJ, Meltzer P (2003) *Nat Rev Cancer* 3:685–694.
19. Lundberg AS, Randell SH, Stewart SA, Elenbaas B, Hartwell KA, Brooks MW, Fleming MD, Olsen JC, Miller SW, Weinberg RA, *et al.* (2002) *Oncogene* 21:4577–4586.
20. Hahn WC, Dessain SK, Brooks MW, King JE, Elenbaas B, Sabatini DM, DeCaprio JA, Weinberg RA (2002) *Mol Cell Biol* 22:2111–2123, and erratum 22:3562.
21. Yeh E, Cunningham M, Arnold H, Chasse D, Monteith T, Ivaldi G, Hahn WC, Stukenberg PT, Shenolikar S, Uchida T, *et al.* (2004) *Nat Cell Biol* 6:308–318.
22. Hanahan D, Weinberg RA (2000) *Cell* 100:57–70.
23. Henderson SR, Guiliano D, Presneau N, McLean S, Frow R, Vujovic S, Anderson J, Sebire N, Whelan J, Athanasou N, *et al.* (2005) *Genome Biol* 6:R76.1–R76.11.
24. Tian WN, Braunstein LD, Pang JD, Stuhlmeier KM, Xi QC, Tian XN, Stanton RC (1998) *J Biol Chem* 273:10609–10617.
25. Dang CV, Semenza GL (1999) *Trends Biochem Sci* 24:68–72.
26. Carmeliet P, Dor Y, Herbert JM, Fukumura D, Brusselmans K, Dewerchin M, Neeman M, Bono F, Abramovitch R, Maxwell P, *et al.* (1998) *Nature* 394:485–490.
27. Semenza GL (2000) *Crit Rev Biochem Mol Biol* 35:71–103.
28. Rubio D, Garcia-Castro J, Martin MC, de la Fuente R, Cigudosa JC, Lloyd AC, Bernad A (2005) *Cancer Res* 65:3035–3039.
29. Serakinci N, Guldberg P, Burns JS, Abdallah B, Schrodder H, Jensen T, Kassem M (2004) *Oncogene* 23:5095–5098.
30. Carew JS, Huang P (2002) *Mol Cancer* 1:9.
31. Gottlieb E, Tomlinson IP (2005) *Nat Rev Cancer* 5:857–866.
32. Shim H, Dolde C, Lewis BC, Wu CS, Dang G, Jungmann RA, DallaFavera R, Dang CV (1997) *Proc Natl Acad Sci USA* 94:6658–6663.
33. Flier JS, Mueckler MM, Usher P, Lodish HF (1987) *Science* 20:1492–1495.
34. Li F, Wang YY, Zeller KI, Potter JJ, Wonsey DR, O'Donnell KA, Kim JW, Yustein JT, Lee LA, Dang CV (2005) *Mol Cell Biol* 25:6225–6234.
35. Warburg O (1930) in *Metabolism of Tumors*, trans Dickens F (Constable, London).
36. Sulis E (1972) *Lancet* 1:1185.
37. Kuo WY, Lin JY, Tang TK (2000) *Int J Cancer* 85:857–864.
38. Pelicano H, Carney D, Huang P (2004) *Drug Resist Updat* 7:97–110.
39. Gambhir SS (2002) *Nat Rev Cancer* 2:683–693.
40. Wang J, Xie LY, Allan S, Beach D, Hannon GJ (1998) *Genes Dev* 12:1769–1774.
41. Zhang Z, Yu J, Stanton RC (2000) *Anal Biochem* 285:163–167.
42. El Emir E, Boxer GM, Petrie IA, Boden RW, Dearling JL, Begent RH, Pedley RB (2005) *Eur J Cancer* 41:799–806.